
S&G 3612

Dense Array Analysis of Ground Motions in a Sedimentary Basin

Jiashun Yu

Institute of Geological and Nuclear Sciences

J.John Taber

Victoria University of Wellington

A report to the NZ Earthquake Commission

October 2000

Table of Contents

Non-Technical Abstract	3
Summary and Technical Abstract	4
Project Introduction	5
Paper: A Correlation between Amplification and Spatial Coherence of Seismic Waves in the Parkway basin, New Zealand	6
1. Introduction	6
2. Observations	6
2.1 Data	7
2.2 Analysis	10
2.3 Results	12
3. 3D Modelling	17
3.1 Model	17
3.2 Modelling	23
3.3 Results	24
4. Discussion	28
5. Conclusions	29
6. Acknowledgements	29
7. References	29

Non-Technical Abstract

The ground shaking experienced on soft sediments during an earthquake is amplified when compared to nearby sites on solid rock. However the level of amplification varies from earthquake to earthquake and the cause of this variation has not been adequately explained. In this project, seismic data from Parkway, Wainuiomata, New Zealand, were used to study the relationship between the variability of seismic amplification by soft soils in a basin and the nature of the seismic waves arriving in the basin. The seismic waves arriving in the basin have been characterised by their coherence, which is a measure of the uniformity of the incoming wave across the basin.

Ten earthquakes that were recorded at the same six soil sites inside the basin and three rock sites surrounding the basin were selected for the study. The resonant frequency at the soil sites was 1.7 Hz and the average amplification of the soil sites relative to the rock sites for all the earthquakes was 8.5. The average amplification of individual earthquakes in the basin was determined to show the variation between earthquakes and this was compared to the coherence of the seismic waves for each earthquake. The results demonstrate that there is a correlation between the amplification and the coherence of the seismic waves at the resonant frequency.

To test the interpretation of the recorded data, three-dimensional computer modelling of the ground motion in the basin was conducted, using different types of seismic waves to approximate different levels of coherence. The modelling supported the correlation found from the observed data and suggests that the more coherent the incoming seismic waves, the greater the ground motion amplification in a sedimentary basin.

Summary and Technical Abstract

Seismic data from Parkway, Wainuiomata, New Zealand, were used to study the relationship between the variability of seismic amplification by soft soils in a basin and the spatial coherence of seismic waves. The basin is a 400 m wide alluvial valley with a depth to basement of up to 65 m. Ten earthquakes that were recorded at the same six soil sites inside the basin and three rock sites surrounding the basin were selected for the study. Using the average seismic spectrum from the three rock sites as a reference, a spectral ratio of each soil site to the rock sites was calculated for each event. The fundamental resonant frequency at the soil sites was 1.7 +/- 0.1 Hz. The fundamental amplification was 8.5 +/- 1.5.

The relative strength of amplification of an earthquake in the basin, defined as the amplification of the event normalised by the average over all the events, was used as an index to show how much the seismic waves were amplified in the basin compared with other earthquakes. The strength of amplification at the fundamental resonant frequency for the ten events ranged from 0.82 to 1.14. Spatial coherence functions of seismic waves recorded at the six soil sites were also calculated for each event. The coherence values at the resonant frequency varied from 0.68 to 0.92 for the ten events. The results demonstrate that there is a correlation between the strength of amplification and the coherence of the seismic waves at the fundamental resonant frequency.

To test the interpretation of the recorded data, three-dimensional computer modelling of the ground motion in the basin was conducted for three types of incident waves. The 3D model of the basin was developed in a two step process. First, the available geotechnical data were used to create three 1D models in different parts of the basin which were adjusted until they approximately matched the resonant frequency and amplification levels of recorded data from nearby sites. Then the 3D model for the basin was built by extrapolating the parameters of the 1D models across the basin.

The seismic waves introduced into the 3D model included normal incidence SH waves, normal incidence SV waves and spatially randomly incident SH and SV waves. The first two represent coherent wavefields and the last represents a randomly incident wavefield. The modelling shows that the pure SH or SV incident waves were amplified significantly more than the random waves. This supports the correlation found from the observed data and suggests that the more coherent the incoming wave field, the greater the ground motion amplification in a sedimentary basin.

Project Introduction

The primary objective of the proposed study has been to examine the effect of the spatial coherence of seismic waves on the ground motion amplification pattern in a sedimentary basin. The research is part of a longer term programme of quantifying the variations in ground motions in population centres so as to allow planners to concentrate hazard mitigation efforts on the areas most at risk.

The study has focussed on the analysis of observed seismic data from Parkway, Wainuiomata, and on 3D computer modelling of the response of the basin to random incident waves.

The specific objectives of the study were to:

1. Determine the correlation of seismic ground motion amplification and the spatial coherence of incident waves from observed data

2. Test the correlation by computer modelling.

These objectives have been met, and the results are described in the following report.

Preliminary results dealing with the analysis of the variability of the amplification within the basin were presented at the annual meeting of the American Geophysical Union in San Francisco in 1998 and the annual meeting of the New Zealand Society for Earthquake Engineering in 1999. The final results of the research will be presented at the annual meeting of the American Geophysical Union in San Francisco in December 2000.

The remainder of the report is in the form of a paper, which has been prepared for submission to the Bulletin of the New Zealand Society for Earthquake Engineering.

A Correlation between Amplification and Spatial Coherence of Seismic Waves in the Parkway basin, New Zealand

Jiashun Yu, Institute of Geological and Nuclear Sciences
J. John Taber, Victoria University of Wellington

To be submitted to: *Bulletin of the New Zealand Society for Earthquake Engineering*

1. Introduction

The amplification of ground motion within sedimentary basins has been a major factor in the damage distribution from some earthquakes (e.g., Hough at el., 1990; Borcherdt and Glassmoyer, 1992; Holzer 1994). Therefore it is desirable for the purposes of earthquake engineering to be able to predict the potential seismic ground motion amplification at a site of interest in a future earthquake. In practice the amplification factor is usually evaluated by using observations of past earthquakes. This would work well if the amplification relative to a reference site were the same for all earthquakes. However observations show that the amplification for a site varies from event to event (Haines and Yu, 1997; Taber and Luo, 1995; Field and Jacob, 1995). Therefore the variability must be understood before the prediction of amplification becomes practically reliable.

Although the variability of amplification of seismic ground motion has been documented in some studies (e.g. Field and Jacob, 1995), not until recently was it suggested that the variability is correlated with the coherence of incident waves (Yu, 1996a). In studying the amplification pattern in the Alfredton basin, New Zealand, Yu and Haines (1994) identified that seismic waves from local events were usually amplified more than the more distant events. Further study showed that the more amplified waves were also more spatially coherent than those that were less amplified (Yu, 1996a; Haines and Yu, 1997). A hypothesis was proposed that the degree of amplification is affected by the spatial coherence of the incident waves, as well as being controlled by the local geology of the observation site (Yu, 1996a). Thus it may be the variable degree of coherence of incident seismic waves for different earthquakes that causes the variability of amplification of seismic ground motion.

3D modelling of random wavefields in the Alfredton basin also exhibited the correlation between the amplification and coherence (Yu, 1996a). However, the Alfredton basin is not typical in that it did not show a strongly resonant behaviour. A case study using a resonant basin is necessary before the correlation can be applied to seismic ground motion for sites with strong amplification. Therefore, the Parkway basin, a typical sedimentary basin with strong seismic amplification in the Wellington area, New Zealand (Taber and Smith, 1992; Yu and Haines, 2000), was selected for studying whether the amplification variability in such a resonant basin is also correlated with the spatial coherence of the seismic waves.

In this paper, the variability of amplifications and the spatial coherence of seismic waves is characterised for 10 earthquakes recorded in the Parkway basin. This enables the determination of the correlation between the amplification and coherence. Then three-dimensional modelling of seismic waves in the basin with different coherences is discussed. The modelling provides a test as to whether the degree of seismic amplification in the basin is correlated with the coherence of the waves.

2. Observations

2.1. Data

Parkway, Wainuiomata, is a suburban residential area of Wellington, New Zealand (Figure 1). It is a flat-floored 400 m wide alluvial valley basin, with a stream running through the centre from the north to the south. The basin floor is about 90 metres above sea level. Taber and Smith (1992) discovered a very large amplification of seismic ground motion in the Wainuiomata area and following that, a dense temporary seismic array was deployed in Parkway in 1995 to study the seismic amplification (Yu, 1996b, Beetham 1999). There were 20 soil sites in the basin and 4 rock sites surrounding the basin that recorded up to 85 events over a 2 month period. The observations revealed that there are two contributions to the very large amplification in the basin, including the resonant amplification in the local soil in the basin and an amplification in the background geological setting (Yu and Haines, 2000). Their study showed that the local resonant amplification provided a factor of about 9±1 at a frequency of 1.7±0.1 Hz. The large variability in amplification between earthquakes that was seen in the original study (Taber and Smith, 1992) was greatly reduced by using the average of four local rock sites as the reference instead of a single reference site 2 km away, however significant variability remained to be explained.

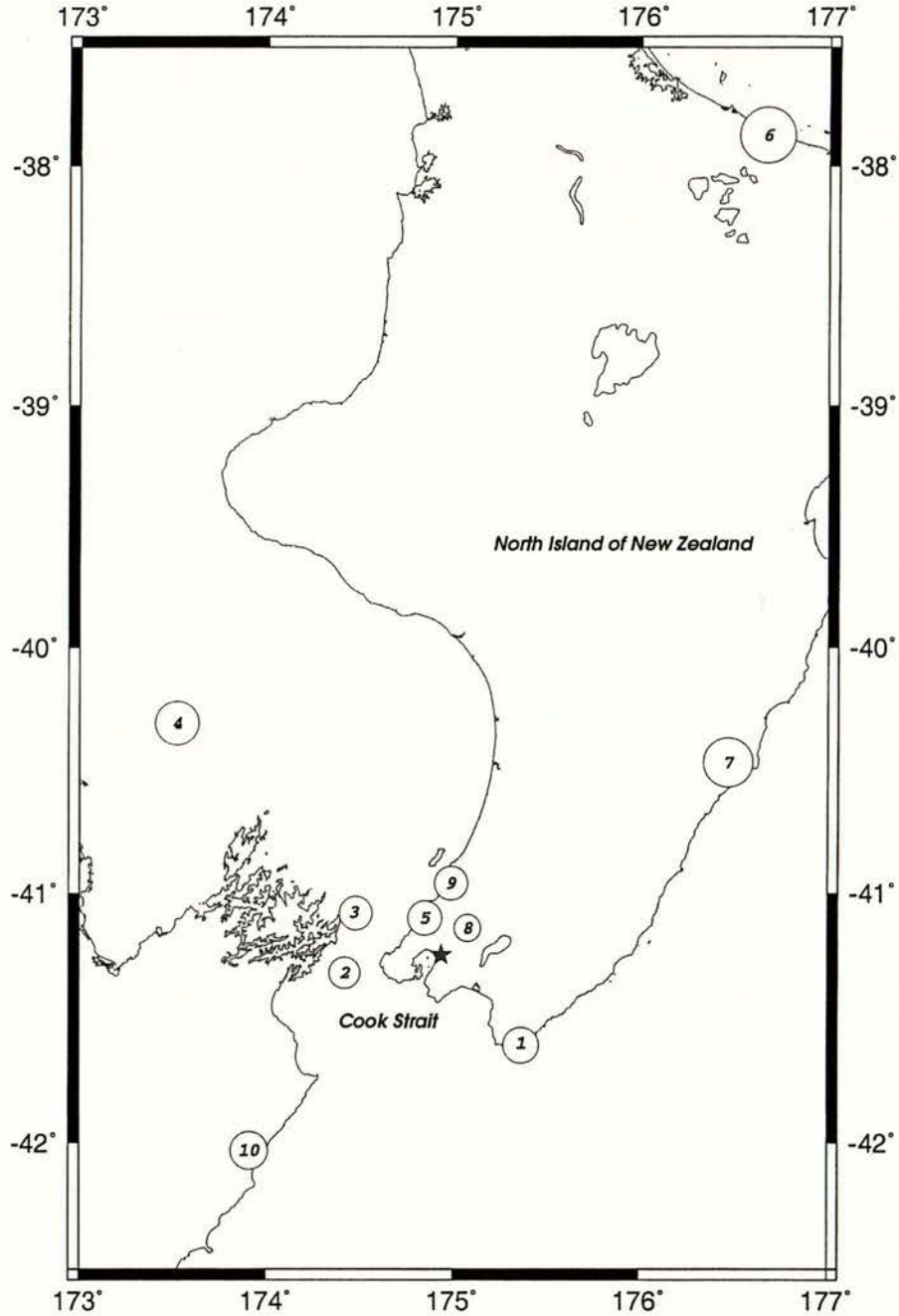

Figure 1 Location of the Parkway basin (star) and the 10 earthquakes (circles) used for this study. The earthquakes were recorded by all 6 soil sites and 3 reference sites (see Table 1 for earthquake parameters).

In this paper we present our study of the the relationship between the local resonant amplification and the spatial coherence of the seismic waves in the Parkway basin. In order to use a uniform set of recordings for the study, 10 earthquakes that were recorded at all six soil sites in the basin and 3 rock sites surrounding the basin were selected from the 1995 data set. The magnitudes of these earthquakes ranged from 2.5 to 5.2 and the hypocentral distances range from 17 to 436 km. The horizontal PGA of the earthquakes observed in the basin ranged from 0.013 to 0.108 m/s^2. The locations of the earthquakes are shown in Figure 1 and Table 1 lists the parameters for each of the earthquakes. The recordings from the rock sites were used as a reference to quantify the amplification in the basin. The 6 soil sites fall into three pairs, with a site separation of about 25 m for each pair. The pairs were selected for the coherence analysis because of the similarity in distance between the two sites in each pair. Having the separation distance for each pair was necessary for consistency in the statistics. The locations of the nine sites used in this study are shown in Figure 2.

Table 1 Parameters of the 10 earthquakes

Num	yr	mo	da	hr	mi	sec	Lat	Long	Depth	Dist	Mag	HPGA
1	1995	08	04	18	15	56.4	41.61	175.37	24	59	3.3	.0023
2	1995	08	05	13	21	52.0	41.32	174.42	40	59	2.9	.0019
3	1995	08	06	12	52	28.2	41.08	174.48	40	58	3.1	.0038
4	1995	08	08	10	04	54.7	40.31	173.52	195	251	4.1	.0041
5	1995	09	03	15	57	37.2	41.10	174.85	56	58	3.2	.0105
6	1995	09	03	17	51	39.2	37.87	176.67	160	434	5.2	.0085
7	1995	09	11	08	53	35.3	40.47	176.47	42	160	4.6	.0085
8	1995	09	12	12	55	39.8	41.14	175.08	5	17	2.5	.0057
9	1995	09	13	14	31	33.2	40.96	174.99	29	43	3.1	.0108
10	1995	09	14	13	45	26.7	42.03	173.91	21	123	3.5	.0013

* Dist = hypocentral distance (km); HPGA = horizontal PGA (m/s^2)

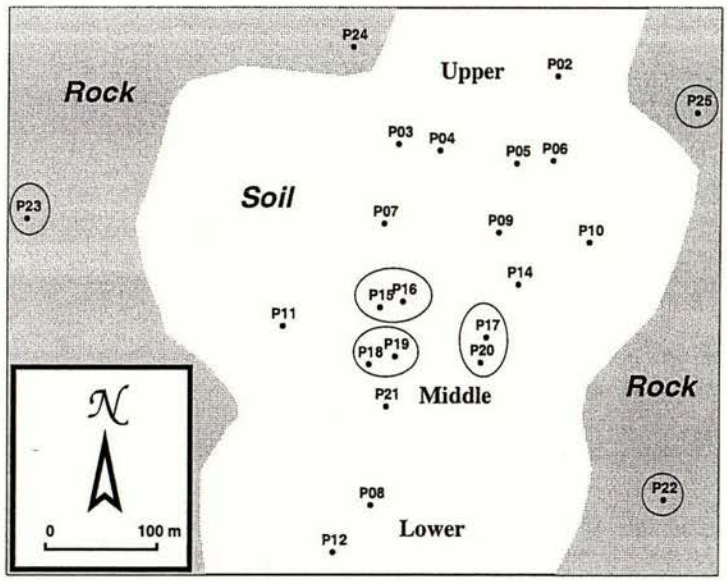

Figure 2 The Parkway Basin and the seismic sites occupied in the 1995 deployment. The circled sites where the ones used for this study. Sites P22, P23 and P25 were on rock (grey shaded area) surrounding the basin. These were used as the reference sites. The other 6 sites were on the flexible soil in the basin. Upper, Middle, and Lower refer to the 3D computer model discussed in Section 3.

2.2. Analysis

The simplest way to quantify the earthquake-to-earthquake variation in amplification at a soil site is to evaluate the range in spectral ratios of that site to the reference sites due to different earthquakes. However a single site is not statistically stable enough to represent the variation in amplification in the basin. Instead, recordings from all the soil sites can be combined to characterise the variation. An average of all the spectral ratios of an earthquake from all sites can be a solution to this. But a direct stacking of the spectral ratios of all the sites is not appropriate because the contribution from each site would be weighted by the amplification at the site. This means that a site with larger amplification would dominate the result. To avoid the unwanted site weighting, the spectral ratio of an earthquake for a site was normalised by the mean of the peak

amplitudes of the spectral ratios for all the events at that site before calculating the average over the sites. Thus the function characterising the variability of amplification for the waves of the jth event is mathematically defined as:

$$S_j(f) = \frac{1}{N} \sum_{i=1}^{N} \frac{R_{ij}(f)}{R_i}$$

where R_{ij} is the soil to rock spectral ratio of the jth event at the ith site. N is the number of soil sites used for studying the amplification strength. For this paper, $N = 6$. R_i is the mean of the peak amplitudes of the spectral ratios of all events at the ith site.

The maxima of the defined function will vary around 1. If there were no variation in amplification from event to event, it would remain 1 for all events. The difference away from 1 reflects the relative amplification of the waves of an earthquake in the basin compared with other earthquakes. In other words the peak amplitude of the function is a factor indicating the relative amplification of the waves of that event. This factor is defined here as the *strength of amplification* or simply the *strength.*

The spectral ratio for the jth event at the ith site was calculated according to the following definition:

$$R_{ij}(f) = \frac{H_{ij}(f)}{\frac{1}{3}\left(H_{22,j}(f) + H_{23,j}(f) + H_{25,j}(f)\right)}$$

where H_{ij} is the RMS of the amplitude spectra of the shear wave parts of the north and east components of the recordings of the ith event at the jth site. Sites P22, P23 and P25 were located on the surrounding rocks and hence were used as the reference.

The spatial coherence of seismic wavefields is defined as the coherence of the same components of recordings at two separate sites:

$$Coh_{ij}(f) = \frac{\left|F_i(f) + F_j(f)\right|^2}{|F_i(f)|^2 + \left|F_j(f)\right|^2} - 1$$

where F_i is the amplitude spectrum of the shear wave part of the north or east component recorded at the ith site and F_j is the amplitude spectrum of the same component at the jth site. The function as defined is non-biased. It equals one when the two components are identical and the expectation of it equals zero when the two are white noise. Therefore the function is a

measure of the similarity of the wave at the two sites. Note that there are three pair of sites in the basin suitable for coherence analysis. As shown in the following sections, the amplification at these sites are similar. Therefore an average can also apply to the coherence functions for these pairs of sites to show the coherence of the waves in the basin.

As the study is focussed on the amplification of the shear waves, the spectral ratios, strength functions of amplification and the coherence functions were all calculated using the shear wave parts of the recordings. The time duration of the series used for calculating the spectral ratios and strength of amplification was 50 seconds starting just before the shear wave arrival. For calculating the coherence functions only the first 6 seconds were used. This is normally the most coherent part of a recording as the later arrivals have too much scattering involved and are less useful for the analysis. Each truncated recording was first tapered by a Hanning window before being used in the calculation. The width of the Hanning window was 2% of the total length of the truncated series. The functions calculated according to the above definitions were finally smoothed using a triangular filter of 0.2 Hz half-width.

The original intention was to evaluate the coherence of the incident waves, not the waves inside the basin, which would be affected by scattering within the basin. Thus it would be ideal if the coherence functions could be calculated using recordings from somewhere in the basement rock where the scattering from the basin would be negligible. Borehole sites beneath the basin, or rock sites outside the basin would meet the requirement. At an early stage of the study coherence functions were calculated using the recordings from the rock sites P22 and P25, but it was found that the coherence between the recordings at these two sites was not significantly better than background noise. This probably was due to the large separation between the two sites (350 m). Wavefields in this area may not be coherent for a separation of this distance. As an alternative the coherence in the following analysis has been calculated using recordings from the 3 pairs of soil sites in the basin. The distance between the two sites in each pair of sites is about 25 metres. The coherence calculated using the recordings from the soil sites inside the basin includes two parts, that of the incident waves and also the scattered waves inside the basin. It is expected that the coherence inside the basin will be lower than the incident wavefield but relative values of the coherence function within the basin should still reflect relative levels of the coherence of the incident waves.

2.3. Results

The amplification of seismic ground motion in the basin is shown by the spectral ratios from the six soil sites relative to the average of the three reference rock sites (Figure 3). The amplification is similar at the six sites. The fundamental resonant frequency is 1.7±0.1 Hz. There is

significant variation in amplification at each site due to different events. This is shown by the mean +/- one standard deviation curves for each site in Figure 3. Note that the event variation range is consistent across all the six sites. Statistics over the sites shows that the peak amplification is 8.5±1.5. The consistency in amplification and event variation range across the six sites suggests that these are appropriate sites for the analysis of the strength and coherence of the seismic waves in the basin.

Note that the spectral ratios, the strength functions and coherence functions in Figures 3, 4 and 5 respectively, are presented in the frequency band of 0.5 Hz to 4 Hz. This effectively covers the resonant frequency in the basin. Frequencies lower than 0.5 Hz are not presented because the seismograms used for the analysis were recorded by the EARSS seismographs with 1 Hz velocity sensors, which have an insufficient system response below 0.5 Hz.

The strength function of amplification in the basin was calculated according to the above definition for each of the 10 events (Figure 4). As can be seen from the figure the range in strength for different stations is small. This implies both that the frequency response at the six soil sites is very similar and that the relative amplification between different events is consistent across all sites (as can also be seen in Figure 3). In some events the ground motion was amplified throughout the basin more than others (e.g., compare Event 5 and Event 4) and this produces the range of values seen in Figure 3.

To examine if event strength was correlated with coherence, the spatial coherence was first calculated for each component of each basin site pair (P15-P16, P17-P20 and P18-P19) for each event. Then the average function for each event was calculated using the six functions for the event (three sites with two components each). The average functions are shown in Figure 5. The figure shows that the variation over pairs of sites of the coherence is relatively small near the resonant frequency, 1.7 Hz, for each individual event. As expected, the coherence decreases at higher frequencies due to shorter wavelengths, but it isn't clear why in a number of cases the coherence decreases at low frequencies.

To find out the relationship between the strength and coherence, the peak strength was read from the strength function for each event (Figure 4) and the coherence value was also read from the coherence functions for each event (Figure 5) at the frequency from where the peak strength was read. The strength ranged from 0.82 to 1.14 and the coherence ranged from 0.68 to 0.92. The correlation between event coherence and strength is shown in Figure 6 along with the standard deviations. Comparing the standard deviations with the ranges of coherence and strength shows that the errors are relatively large. However there is a clear correlation shown by the mean values between strength and coherence, with strength increasing with coherence. This means that those waves that are spatially more coherent tend to be amplified more in the basin.

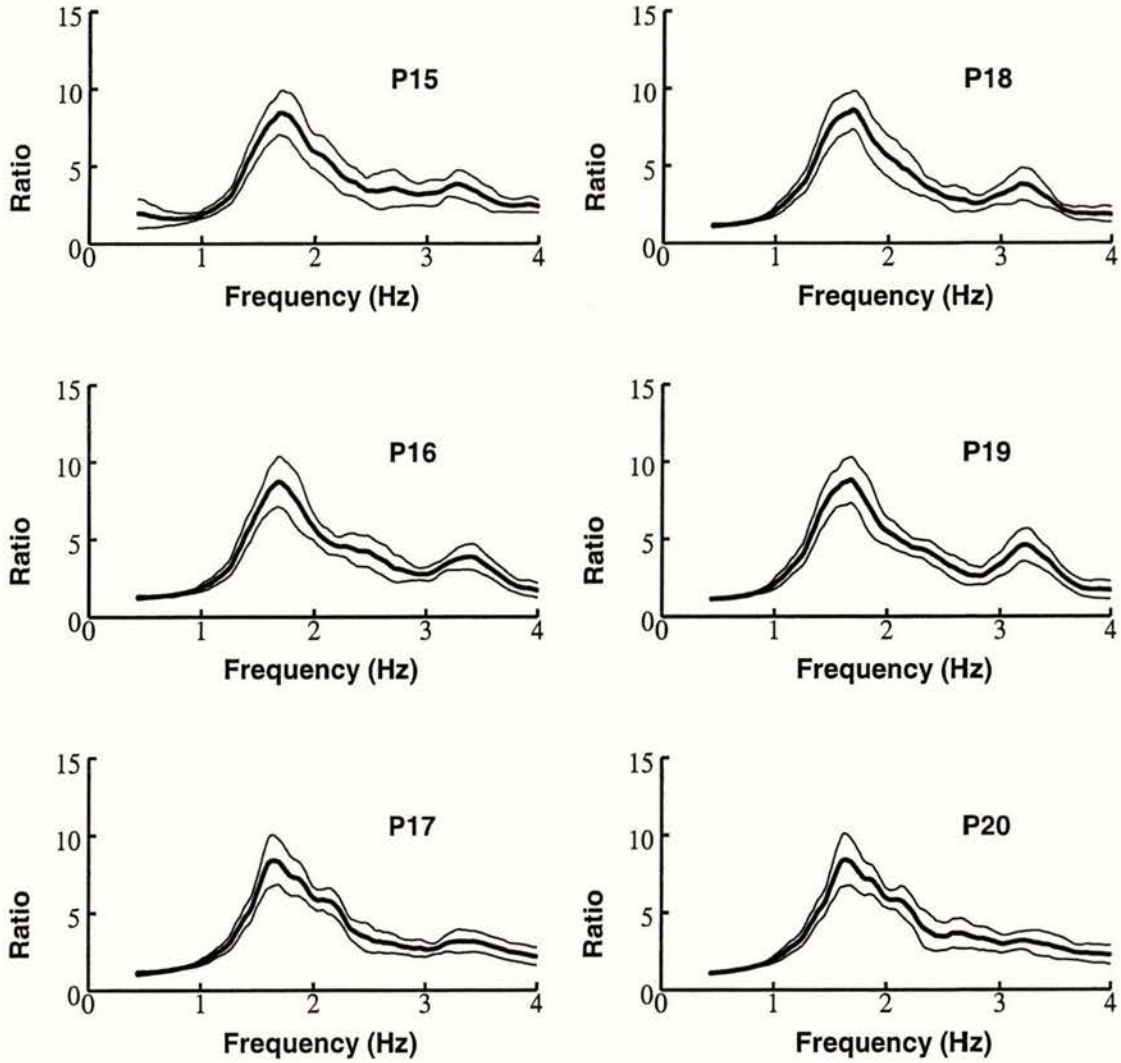

Figure 3 The spectral ratios of the six basin sites relative to the average of the three reference rock sites. The dark line is the mean ratio of all events and the two thin lines are +/- one standard deviation. A 50 second sample starting just before the S wave was used for each spectrum. Each spectrum was smoothed using a 0.2 Hz half-width triangular moving window. The amplification is similar at the six sites. The fundamental resonant frequency and amplification are 1.7±0.1 Hz and 8.5±1.5, respectively. Note the significant variability in the spectral ratio between events at each site.

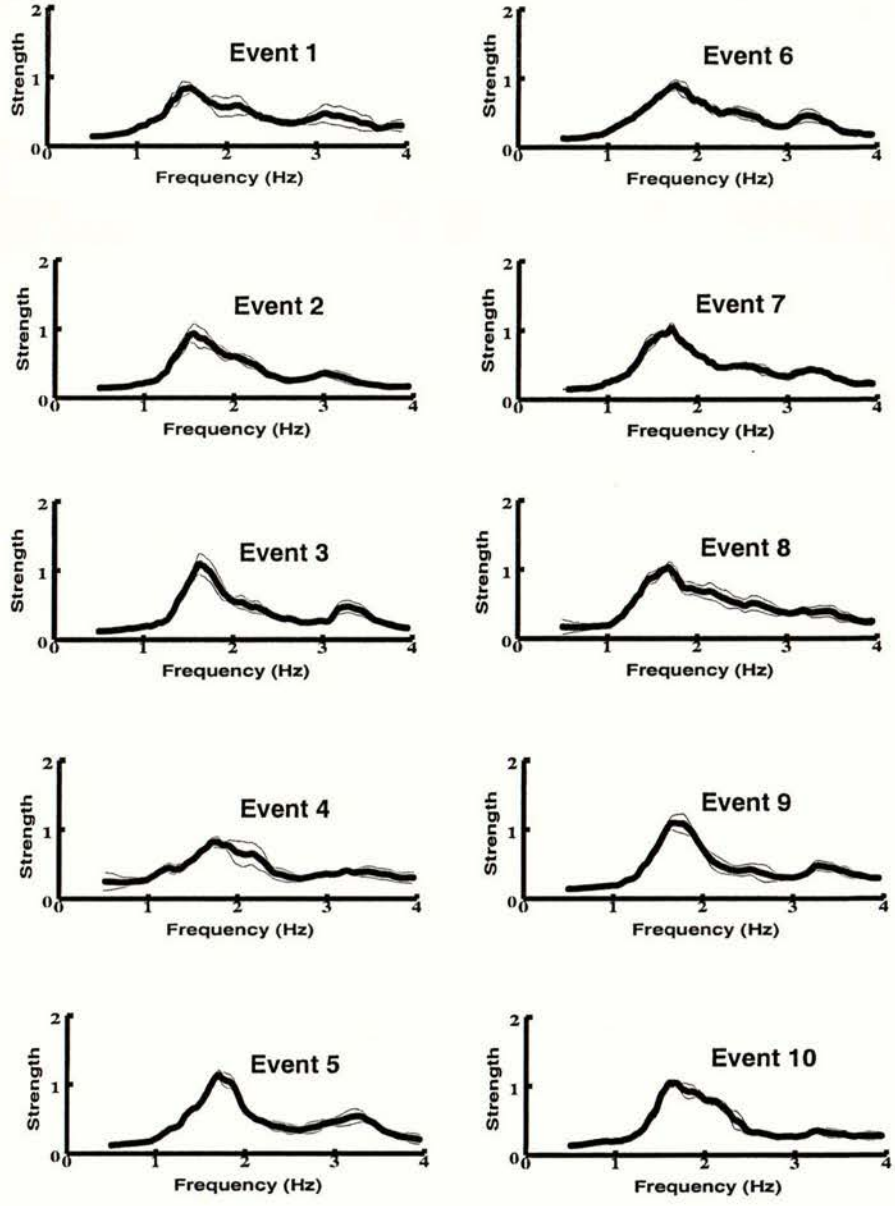

Figure 4 Strength of amplification for each event. The thick curve for each event is the mean strength over the 6 soil sites, while the thin curves show the range of strengths at the six sites for a particular event (mean +/- one standard deviation). The peak strength for each event occurs close to the fundamental resonant frequency of 1.7 Hz. These peaks range from 0.82 (Event 4) to 1.14 (Event 5). Note the small standard deviations and the larger range of strengths between events.

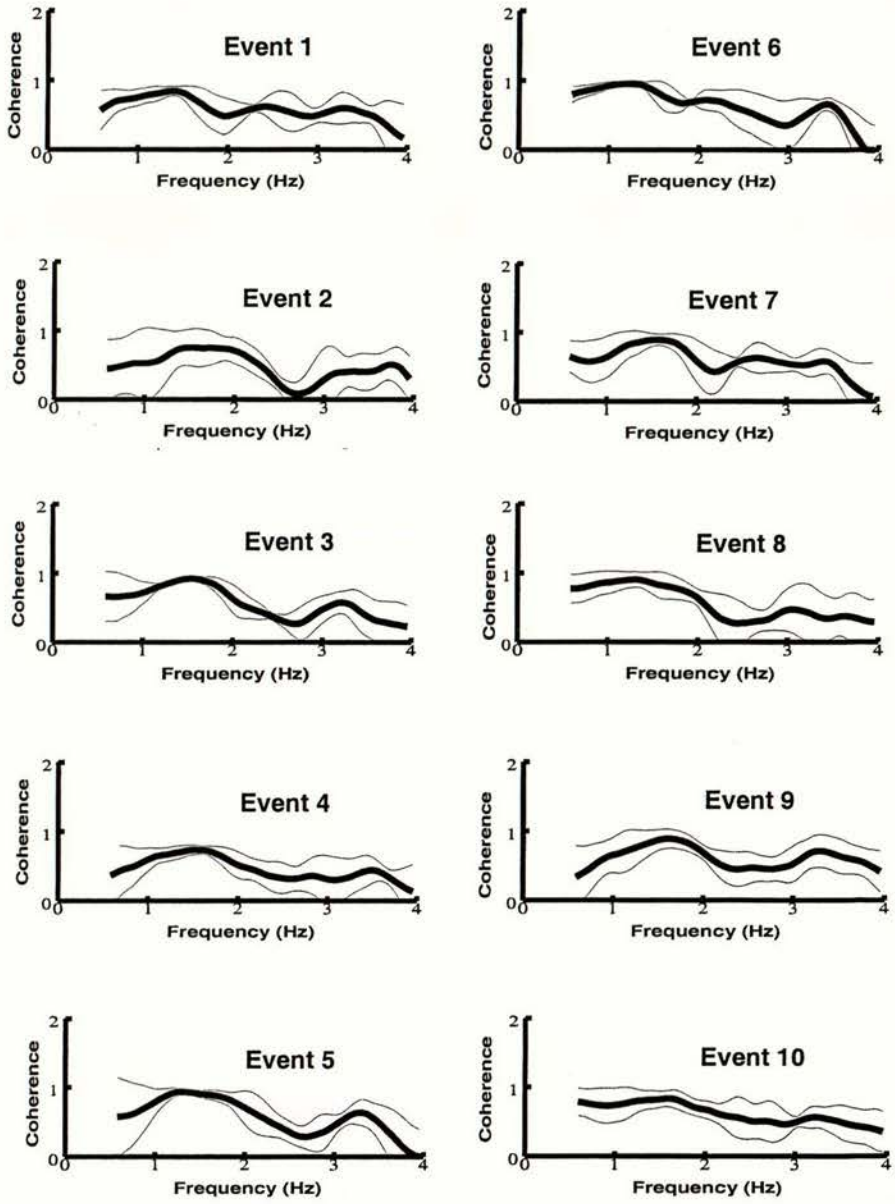

Figure 5 The average spatial coherence of the seismic waves for the 10 earthquakes. The thick lines are the means of the 2 horizontal components for the 3 pairs of sites for each event. The thin curves are the mean +/- one standard deviation.

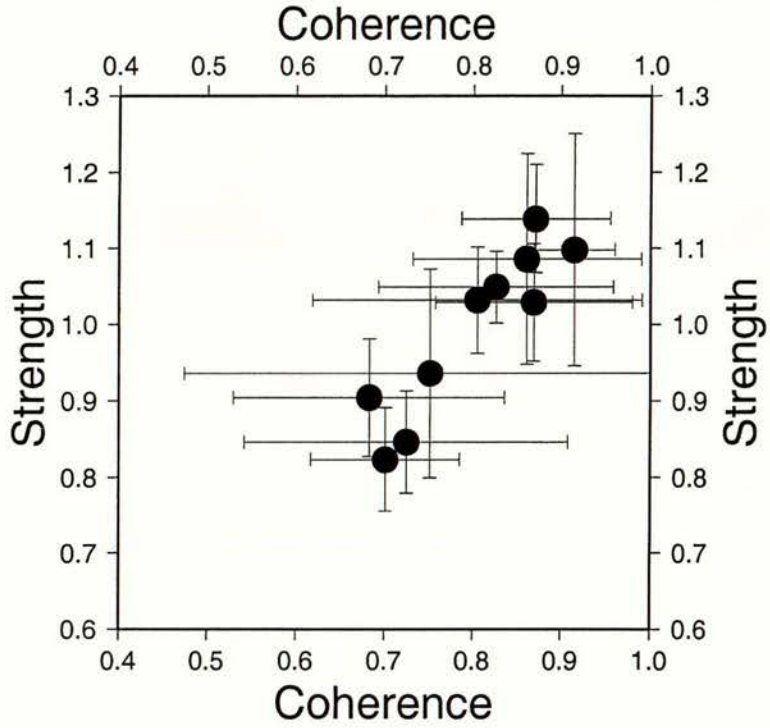

Figure 6 Correlation between spatial coherence and the strength of amplification of the seismic waves. Filled circles show the strength and mean coherence for each event. Bars show +/- one standard deviation of both parameters. The mean values range from 0.82 to 1.14 for strength and 0.68 to 0.92 for coherence. There is a clear correlation between the strength of amplification and spatial coherence of the seismic waves at the fundamental frequency.

3. 3D Modelling

3.1. Model

A series of geotechnical investigations carried out in the Parkway basin and the adjacent Wainuiomata area have been used to help constrain a three dimensional model of the basin, which was then used to calculate seismic waves to study the relationship between the amplification and spatial coherence of the waves. As part of a paleoenvironmental research project, a stratigraphic hole was drilled at a location about 1.5 km southeast of Parkway in 1991. It revealed that there are

61.6 metres of Quaternary deposits above the greywacke basement (Begg et al, 1993). Following the discovery by Taber and Smith (1992) of a very large seismic amplification in Wainuiomata, efforts have been taken to understand the structure and physical parameters of the subsurface materials in the the Parkway basin. Cone penetrometry (CPT) measurements at 11 sites reached depths ranging from 4.5 to 16 metres (Barker, 1996). The fact that the penetrometry could not go deeper indicates a difference in the material composition of the sediments, though the physical parameters beyond this depth remain unknown. Shear wave velocity measurement in 3 of the CPT sites showed that the shear wave velocity varies from 84 to 260 metres per second within the thickness penetrated. Sutherland and Logan (1998), using the method of spectral analysis of surface waves (SASW), also found that the shear wave velocity was about 98 to 250 m/s and density was 1.7 to 1.9 g/cm^3 above the depth of 17.5 metres. Their study also suggested a shear wave velocity of 400 m/s for the depth below this, but the reliability of this estimate is limited. Duggan (1997) used seismic refraction and gravity methods to determine that the basement depth could be up to 70 metres. He suggested a shear wave velocity of 140 to 190 m/s and P wave velocity of 1670 m/s for the Quaternary sediments in the basin.

Table 2 Dominant amplification factors in the Parkway Basin

Site	Freq (Hz)	Amplification factors	
		Mean	Standard deviation
P02	2.1	6.1	0.5
P03	2.6	4.9	1.0
P04	2.2	5.4	1.1
P05	1.8	9.5	1.9
P06	1.9	9.6	2.2
P07	1.9	7.1	1.1
P08	1.4	8.3	1.0
P09	1.7	10.0	1.7
P10	2.1	8.6	1.9
P11	1.7	7.0	0.8
P12	1.4	11.4	1.5
P14	1.7	9.2	1.6
P15	1.7	8.5	1.4
P16	1.7	8.8	1.5
P17	1.7	8.1	1.4
P18	1.7	9.0	1.3
P19	1.6	8.6	1.5
P20	1.6	7.9	1.2
P21	1.5	8.1	1.0

* quoted from Yu and Haines (2000)

These results lack the resolution to constrain a detailed three-dimensional model for the basin. Instead a simple two layer model was developed using the above results as a starting point. As limited data were available to constrain the bottom layer, it was described by using a simple

homogeneous medium. The undetermined physical parameters for the layers, including density, shear wave velocity and the quality factor for shear waves, as well as the depth of the interfaces of the layering, were determined by one-dimensional SH wave modelling (see Yu, 1996a, for the method) with observed resonant frequencies and amplitudes as constraints. The modelling was performed at three indicative sites which represent the upper, middle and lower parts of the stream (from the north to the south, see Figure 2 for locations) in the basin. Recordings of earthquake resonant frequencies and amplitudes from nearby observation sites (Table 2) were used to determine the resonant parameters for the indicative sites (Table 3) that in turn were used as constraints for the 1D SH modelling. A series of parameter models for each indicative site were tested. The one producing the best fit with the constraint was chosen for the site. These parameter models for the indicative sites are listed in Table 4. As modelling outputs, the amplitude response functions due to incident SH waves at the sites are shown in Figure 7.

Table 3 Constraint parameters for 1D SH modelling

Sites	Freq(Hz)	Amplification factor	Interpreted from
Upper	2.5	6	P02-P04
Middle	1.7	9	P15-P20
Lower	1.4	10	P08 & P12

Using the one dimensional models determined at these three sites, a three dimensional model for the basin was built by interpolating and/or extrapolating the parameters of the one dimensional models across the basin. The three dimensional model is 700 by 700 metres laterally, and 68 metres in thickness. The top layer has a thickness of 1 to 16 metres, with a shear wave velocity of 100 to 220 m/s and density of 1.7 to 1.9 g/cm^3. The shear wave velocity and density for the homogeneous bottom layer are 500 m/s and 2.0 g/cm^3, respectively. The full set of physical parameters for the model are listed in Tables 5-7 and the layer thicknesses are shown in Figure 8. The parameters for the top layer are variable. Both the density and shear wave velocity for the layer increase from south to north (Tables 6 and 7), reflecting the variation of the sediments from the lower part of the stream to the upper part. In building the model, the P wave velocity was based on the previous technical data, while the P wave quality factor was based on comparisons with other areas. The geometry and the physical parameters of the model were first digitised at a grid with 50 metre spacing as shown in Tables 6 and 7. Later it was interpolated to be 8.75 metre spacing using a two-dimensional spline method before the modelling was performed.

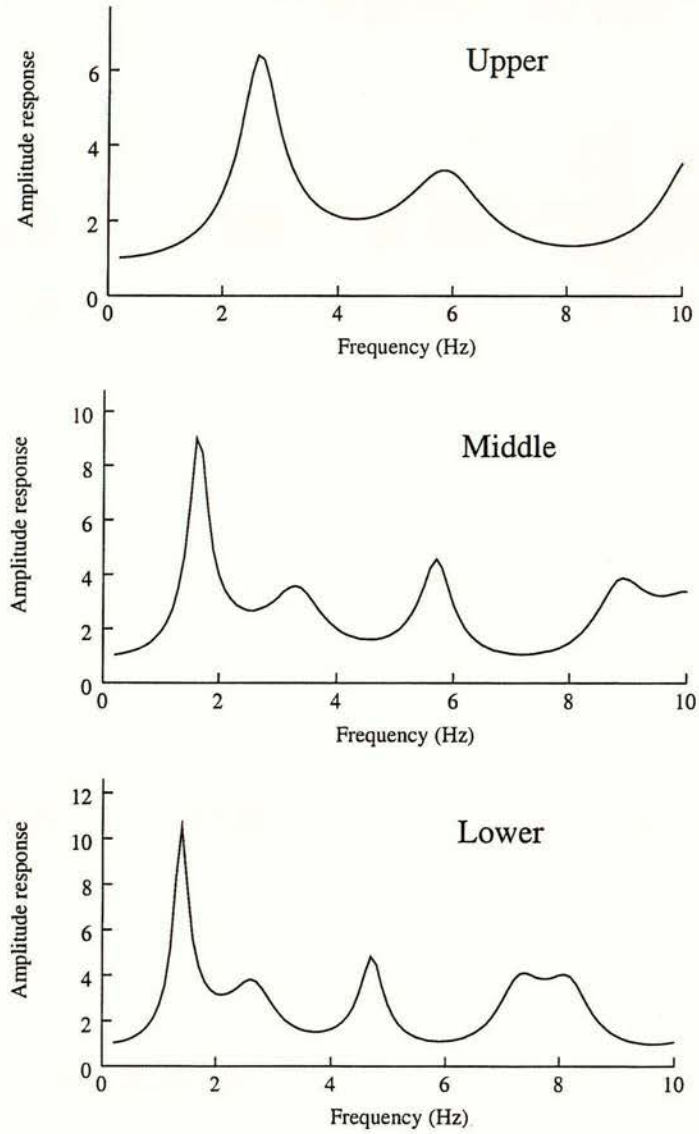

Figure 7 Spectral response of the 1D models used to create the 3D basin model. The upper model approximates the response at sites P02 to P04, the middle at sites P15 to P20, and the lower at sites P08 and P12. Note that the vertical scales vary between plots. See Figure 2 for the location of the sites.

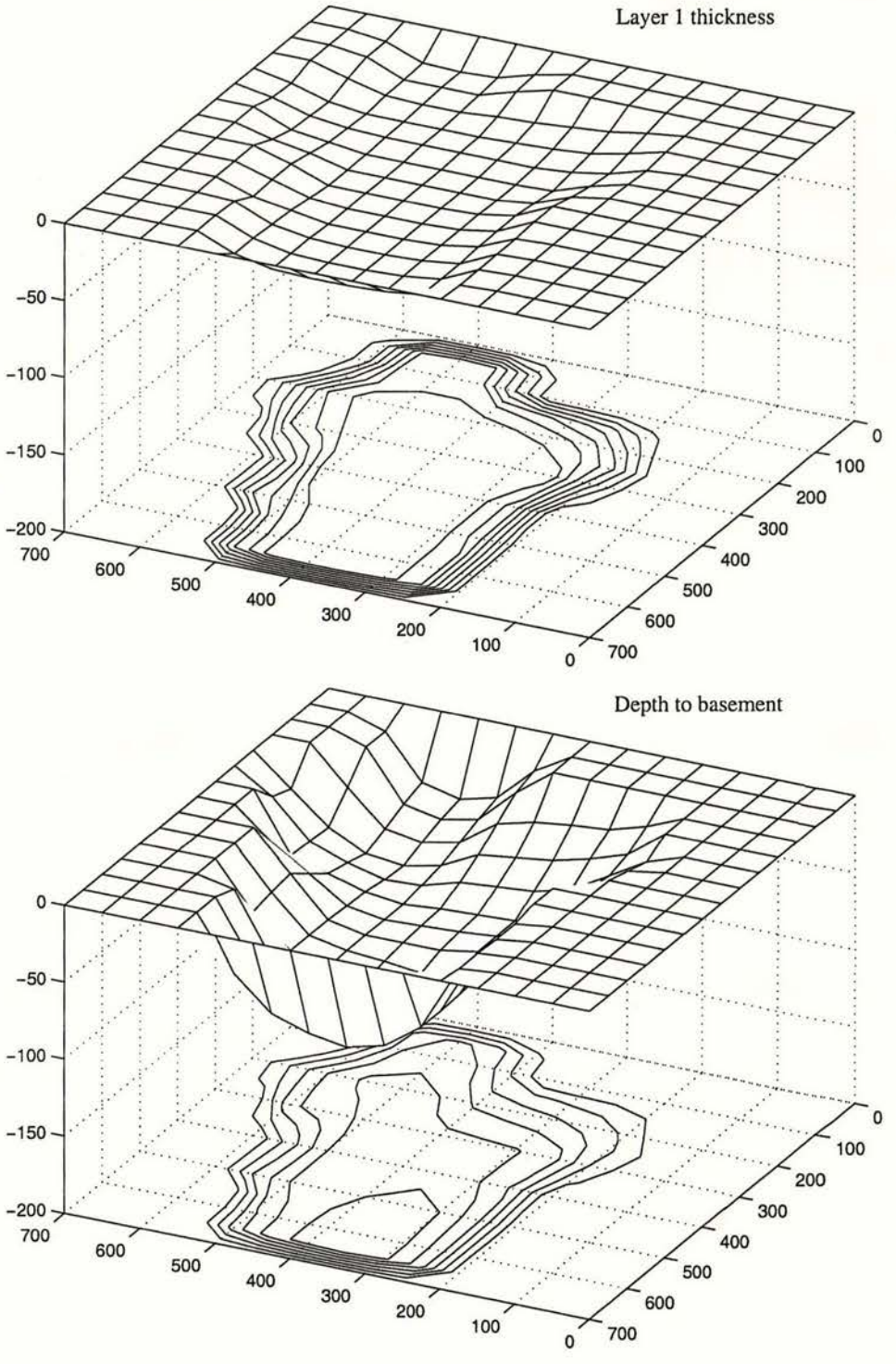

Figure 8 Model geometry. A contour plot is shown at the bottom of each box. Top: bottom interface of Layer 1, contour interval 2 m. Bottom: depth to basement, contour interval 10 m.

Note that the purpose for the 3D modelling was to study the correlation between the amplification and spatial coherence of seismic waves rather than to precisely match the observed amplification pattern. If a matching of amplification patterns was the goal, then the observed resonant frequencies and amplitudes should not have been used as constraints in a 1D modelling to determine the parameters for the 3D model. However in this case it is logically proper, as this produced a 3D model which yields a synthetic amplification pattern similar to the observations, without automatically leading to the same amplification-coherence correlation with the observations.

Table 4 Parameters for the 3 1D models

Sites	Layer	Depth	Velocity	Q	Density
Upper	Top layer	0.0	200	15	1.9
	Bottom layer	15.0	500	50	2.0
	Basement	38.0	1500	300	2.6
Middle	Top layer	0.0	120	15	1.8
	Bottom layer	16.0	500	50	2.0
	Basement	55.0	1500	300	2.6
Lower	Top layer	0.0	100	15	1.7
	Bottom layer	16.0	500	50	2.0
	Basement	65.0	1500	300	2.6

* Depth=the depth of the top interface of the layer.

Table 5 Physical parameters for Parkway basin

Layers	dens(g/cm^3)	Vs(m/s)	Vp(m/s)	Qs	Qp
Top layer	1.7-1.9	100-220	1500	15	50
Bottom layer	2.0	500	2000	50	100
Basement	2.6	1500	3200	inf	inf

* Dens and Vs variable for top layer. See Tables 5 and 6 for details.

Table 6 Density (g/m^3) for the top layer

y\x	0	50	100	150	200	250	300	350	400	450	500	550	600	650	700
0									1.9	1.9	1.9	1.9	1.9		
50									1.9	1.9	1.9	1.9	1.9		
100									1.9	1.9	1.9	1.9	1.9		
150					1.9	1.9	1.9	1.9	1.9	1.9	1.9	1.9	1.9		
200					1.9	1.8	1.8	1.9	1.9	1.9	1.9	1.9	1.9	1.9	
250				1.9	1.8	1.8	1.8	1.8	1.8	1.8	1.8	1.8	1.8	1.9	
300				1.9	1.8	1.8	1.8	1.8	1.8	1.8	1.8	1.8	1.9		
350					1.9	1.8	1.8	1.8	1.8	1.8	1.8	1.8	1.9		
400						1.9	1.8	1.8	1.8	1.8	1.8	1.9			
450						1.9	1.8	1.8	1.8	1.8	1.8	1.9			
500					1.9	1.7	1.7	1.7	1.7	1.7	1.7	1.9			
550					1.9	1.7	1.7	1.7	1.7	1.7	1.7	1.9			
600					1.9	1.7	1.7	1.7	1.7	1.7	1.9				
650						1.9	1.7	1.7	1.7	1.7	1.9				
700						1.9	1.7	1.7	1.7	1.7	1.9				

Table 7 Shear wave velocity (m/s) for the top layer

y\x	0	50	100	150	200	250	300	350	400	450	500	550	600	650	700
0									220	220	220	220	220		
50									220	220	220	220	220		
100									210	210	210	210	210		
150					210	210	210	210	210	210	210	200	200		
200					200	200	200	200	200	190	160	160	160	160	
250				200	200	170	140	140	140	130	130	130	130	130	
300				200	180	160	120	120	120	120	120	120	120		
350					180	160	120	120	120	120	120	120	120		
400						130	120	120	120	120	120	120			
450						120	120	120	120	120	120	120			
500					110	110	110	110	110	110	110	110			
550					100	100	100	100	100	100	100	100			
600					100	100	100	100	100	100	100				
650						100	100	100	100	100	100				
700						100	100	100	100	100	100				

3.2. Modelling

The purpose of the modelling was to test if there is a correlation between the amplification and coherence of the waves in the basin. Therefore two kinds of wavefields were separately synthesised, one representing a coherent case and the other a random case. This provided a comparison of the amplification relative to the coherence of the waves. Incident pure SH and SV waves were separately used as the coherent case, and the superposition of random SH and SV incident

waves from all spatial directions as a random case. The modelling of the random wavefields in a basin was a two step process. First a set of deterministic fundamental wavefields in the basin were calculated. Then these wavefields were randomly combined according to the possible incidence distribution to mimic the random superposition of the wavefield in the basin due to random incident waves (see Yu, 1996a for the details of the method for modelling spatially random wavefields in basins). The wavefields in the basin due to pure SH (or SV) incident waves from a certain spatial direction can be calculated as one of the fundamental wavefields. The Riccati-Haines approach (Yu, 1996a; Haines et al, 2000) was used for modelling the fundamental wavefields. The modelling was performed in a limited discrete wavenumber space defined on the lowest 69 wavenumbers, with the minimum wavenumber to be zero (normal incidence) and a wavenumber increment determined by the dimension of the model, the medium velocity and the frequency of the waves to be modelled. Thus there were 69 plane waves in each fundamental wavefield which was due to either a SH, SV or P incident wave from a certain spatial direction. As the wavenumbers for the incident waves were also defined on the wavenumber space of 69 wavenumbers, theoretically there were 69×3 fundamental wavefields. However as our interest was to model the shear wave part of the observed wavefields, the incident P waves were not considered. Therefore the number of fundamental wavefields were 69×2 for each frequency. These were the set of fundamental wavefields that the random wavefields were composed from.

Although incident waves can enter the basin from any spatial direction, it is more likely that the energy would mainly be from the normal direction with a decrease in energy as the incident angle increases. The reason for this assumption is that the basin is on the ground surface and the shear wave velocity in its basement is relatively low compared with that at the source depths of the earthquakes observed. Therefore the random weights for the random combination were generated in such a way that the random incident waves were mainly from incidence angles of less than 60 degrees, and their energy decreased as the incident angle increased. As the details of the random modelling are beyond the scope of this paper, interested readers are recommended to refer to Yu, 1996a. The modelling was performed for 6 frequencies ranging from 1.5 to 2.0 Hz, with an increment of 0.1 Hz. This covers the resonant frequency of 1.7±0.1 Hz in the basin (Yu and Haines, 2000).

Note that the basin is not totally confined by the greywacke basement, but opens to both the north and south. In order to absorb the reflection from the numerical boundary of the basin at these two sides, low quality factors for both the P and S waves were assigned to these edges of the model. The values of these quality factors were Qs=Qp=2.

3.3. Results

Shown in Figure 9 is the comparison of the amplification patterns of the wavefields in the basin due to different incident waves. The response wavefields in the basin due to each pure type of incident wave are seen to be dominated by the incident wave polarisation. Converted waves are also seen in the basin in the other components, but their amplitudes are relatively small. For

example for the incident SH wave, the resulting amplitude in the Y direction is about 4 times the amplitude in the X direction. For the waves due to random incident waves, the energy is evenly distributed in the two horizontal components. Comparing the random waves with those due to pure types of incident waves, the amplitude of the waves in the basin due to random wavefields is significantly smaller. In other words, the randomness in the incident waves tends to reduce their amplification in the basin.

In order to compare the model results with the recorded data, the amplification and coherence of the synthetic waves were calculated as the average over a 4*4 grid in the central basin where the six observed sites were located. The spacing of the grid was 26.25×26.25 m. This spacing is similar to that of the pairs of soil sites at which the observed data were used for calculating the coherence functions. The average amplification and coherence functions for each synthetic wavefield are listed in Table 8 for each of the calculated frequencies. The first 4 columns show the amplification and coherence of the pure SH and SV waves and the last two columns show the results of the random incidence waves. The table shows that the wavefields due to pure SH or SV incidence are highly coherent in the dominant components, and these components are also largely amplified in the basin compared with the random wavefield. This contrast between the two kinds of wavefields is largest at the resonant frequency of 1.7 Hz. The contrast at this frequency is shown in Figure 10. This modelling result is consistent with the observed correlation between coherence and strength of amplification.

Table 8 Amplification strength and coherence of waves in the Parkway basin

		SH (0)		SV(0)		SH+SV(60)	
Hz		x	y	x	y	x	y
1.5	Coh	0.357	0.996	0.999	0.590	0.964	0.940
	Amp	0.258	7.638	7.506	0.297	4.071	3.821
1.6	Coh	0.357	0.992	0.999	0.354	0.956	0.924
	Amp	0.484	10.652	11.520	0.369	6.150	5.348
1.7	Coh	0.402	0.985	0.995	0.231	0.937	0.899
	Amp	0.886	13.113	15.093	0.697	8.026	6.633
1.8	Coh	0.505	0.963	0.978	0.607	0.901	0.862
	Amp	1.512	12.249	12.937	1.196	6.941	6.264
1.9	Coh	0.473	0.887	0.9616	0.759	0.853	0.796
	Amp	1.844	9.418	10.4622	1.529	5.745	4.877
2.0	Coh	0.373	0.784	0.959	0.624	0.837	0.680
	Amp	1.593	5.700	8.893	1.348	5.033	3.273

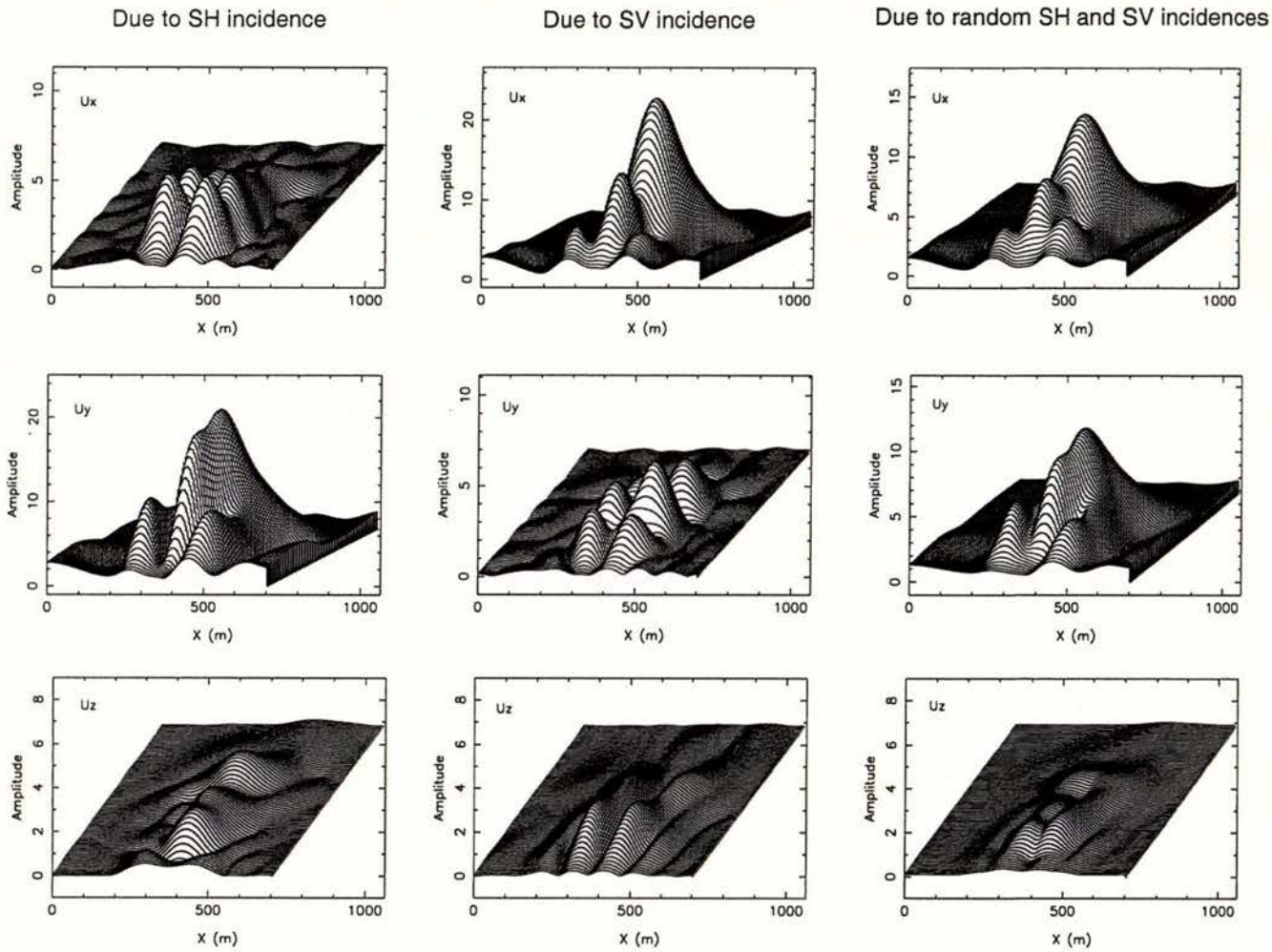

Figure 9 The amplitude of the synthetic wavefields at the ground surface of the basin due to different incident waves at 1.7 Hz. The first column is that due to normal incident SH waves. The second column is that due to normal incident SV waves. The third column is that due to random incident waves of SH and SV types from all spatial directions with various incident angles. There are three blocks in each column. From the top to the bottom, each block shows the x (east), y (south) and z (upward) components. The normal incident SH and SV waves are defined to be polarised in the y and x components, respectively. Note the varying amplitude scales in the plots.

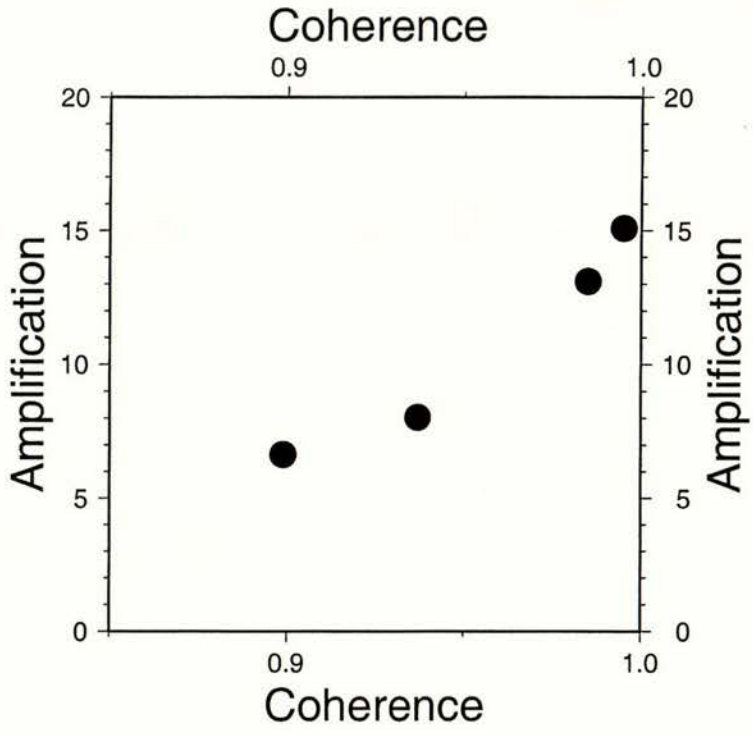

Figure 10 Comparison of the relationship between coherence and amplification for the dominate component of the pure SV and SH incident waves and and the random incidence waves for the 3D model. The values shown are from Table 8 at 1.7 Hz, which is the resonant frequency of the basin.

Note that the basin model for the 3D modelling was constrained using observed resonant amplification factors. The resonant frequency from the three dimensional modelling is 1.7 Hz, which is the same as the constraint. However the amplification in the 3D model at this frequency differs from the 1D case. If there were no three dimensional effect, the amplification due to the highly coherent SH incidence output by the 3D modelling should be similar to the 100% coherent SH waves of the 1D modelling. But this is not the case. The 3D modelling output of amplification is 13.113 at 1.7 Hz due to SH incidence (Table 8). This is significantly greater than the 1D modelling output of about 9. This difference may be due to the focusing effects that can't be included in the 1D modelling. Thus the ground motion at a site in a three dimensional basin is larger than would be shown by 1D modelling. Chávez-Garcĭa et al (1999) have also shown that there are significant 2D effects in the basin. However this does not have significant impact on our study of the correlation between the amplification and coherence.

4. Discussion

It was observed from the recorded earthquakes that highly coherent waves were amplified more in the basin than waves of less coherence. 3D modelling of pure and random wavefields also shows that this is the case. This difference in amplification for the waves of different coherence may be due to the destructive interference of the random waves propagating inside the basin. The resonant amplification in the soil layer is due to the superposition of the waves bouncing back and forth between the ground surface and the basement, and when the waves are in phase, the superposition will produce a greater amplification. The complex random waves have less chance to be in phase and to produce the same amplification as the coherent waves do. Therefore we see that the coherent waves are amplified more in a basin than random waves.

The degree of incoherence, or randomness, of the incident waves may be due to the scattering along the path. The scattering may produce complex secondary waves as well as reducing the dominant contribution of the original waves in the total wavefield. This would result in the decrease of coherence in the total incident wavefield. The more scattering the incident waves experience, the less they are coherent, and hence the less they would be amplified in a basin. Thus the scattering along the path may influence the amplification in a basin. If the degree of scattering is dependent on path length, the incident waves from a very local earthquake would tend to be amplified more than from a distant earthquake, as they would experience less scattering along the short path. Haines and Yu (1997) showed in the case of the Alfredton basin that the wavefields from distance earthquakes were less coherent than from nearby earthquakes. Thus using distant events to estimate the amplification of a site may underestimate the amplification for some local events.

Difference in spatial coherence may not be the sole cause for variability in amplification. Amplification may also be affected by the earthquake source-time function. Haines and Yu (1997) found that simple waves with short duration pulse also tended to be amplified more in the Alfredton basin than complex long duration waves. Therefore a further study taking into account the spatial coherence and the nature of the source function may provide further understanding of the event variability in amplification of seismic ground motion in basins.

Although a correlation between the strength and coherence was shown by the mean values, it cannot be interpreted that the amplification would strictly increase as the coherence increases, because as can be seen from Figure 6, the errors are relatively large. However the correlation from the observations gives some confidence that waves having a big difference in spatial coherence will be amplified differently in the basin. This is supported by the modelling.

5. Conclusions

A correlation between the amplification and spatial coherence in the observed seismic data from the Parkway basin has been found and the correlation is supported by three dimensional computer modelling. The modelling reveals that highly coherent waves tend to be amplified significantly more in a resonant basin than random waves. Based on the analysis of both the observed and synthetic data, it can be concluded that the amplification of seismic waves in the highly resonant Parkway basin is correlated with the spatial coherence as was shown in the less resonant Alfredton basin. The implications of this result are that waves from a local earthquake may tend to be amplified more than a distant earthquake, as the waves from a local earthquake would experience less scattering on their short path to the observation site and hence they would be more coherent.

Acknowledgements

This study has been funded by the EQC Research Foundation. Thanks are due to FRST for funding the data collection and initial analysis. The authors also thank John Haines of Cambridge University for his advice on the three dimensional modelling.

References

Barker, P. R. (1996). A report on cone penetrometer and seismic cone penetrometer testing at Parkway -- Wainuiomata. Barker Consulting, P. O. Box 27-106, Wellington, New Zealand.

Beetham, R. D. (1999). Microzoning project Parkway Basin subsurface investigations, Wainuiomata. Institute of Geological & Nuclear Sciences science report 99/14.

Begg, J. G., Mildenhall, D. C., Lyon, G. L., Stephenson, W. R., Funnell, R. H., Van Dissen, R. J., Bannister, S., Brown, L. J., Pillans, B., Harper, M. A., and Whitton, J. (1993). A paleoenvironmental study of subsurface Quaternary sediments at Wainuiomata, Wellington, New Zealand, and tectonic implications. New Zealand Journal of Geology and Geophysics, (36) 461-473.

Borcherdt, R. D. and G. Glassmoyer (1992). On the characteristics of local geology and their influence on ground motions generated by the Loma Prieta earthquake in the San Francisco bay region, California, *Bull. Seism. Soc. Am. 82*, No 2, pp. 603-641.

Chávez-Garcĭa, F. J., W.R. Stephenson and M. Rodrĭguez (1999). Lateral propagation effects observed at Parkway, New Zealand. A case history to compare 1D versus 2D site effects, *Bull. Seism. Soc. Am. 89*, pp. 718-732.

Duggan, E. B. (1997). Shallow seismic structure of Parkway Basin, Wainuiomata, New Zealand. B. Sc. (Hons) thesis, School of Earth Sciences, Victoria University of Wellington, New Zealand. 1997. p. 116.

Field, E. H., and K. H. Jacob (1995). A comparison and test of various site-response estimation techniques, including three that are not reference-site dependent, *Bull. Seism. Soc. Am. 85*, pp. 1127-1143.

Haines, A. J. and Jiashun Yu (1997). Observation and synthesis of spatially-incoherent weak-motion wavefields at Alfredton Basin, New Zealand. Bulletin of the New Zealand National Society for Earthquake Engineering, Vol. 30, No 1, pp. 14-31.

Haines, A. J., Jiashun Yu and Tom Hulme (2000). Use of generalised invariant imbedding approach in computing seismic wavefields in basins, (in preparation).

Holzer, T. L. (1994). Enhanced ground shaking, *EOS, Transactions of the American Geophysical Union, 75*(26), pp. 299-301.

Hough, S. E., R. D. Borcherdt, P. A. Friberg, R. Busby, E. Field and K. H. Jacob (1990). The role of sediment-induced amplification in the collapse of the Nimitz freeway during the October 17, 1989 Loma Prieta earthquake, *Nature 344*, pp. 853-855.

Sutherland, A. J., and Logan T. C. (1998). SASW Measurement for the Calculation of site amplification. EQC research project 97/276. Central Laboratories Report 98-522422, Opus Institutional Consultants, Lower Hutt, New Zealand.

Taber, J.J., and X. Luo (1995). Uncertainties in site response estimates, Proc. Pacific Conf. Earthquake Engineering, Melbourne, November, 1995, v2, pp. 69-78.

Taber, J. J. and E. G. C. Smith (1992). Frequency dependent amplification of weak ground motions in Porirua and Lower Hutt, New Zealand, *Bull. New Zealand National Society for Earthquake Engineering, 25*, No. 4, pp. 303-331.

Yu, Jiashun (1996a). Observation and synthesis of seismic wavefields in basin structures, PhD thesis, Victoria University of Wellington.

Yu, Jiashun (1996b). Processing of data from a seismic experiment in Parkway, Wainuiomata. Institute of Geological & Nuclear Sciences science report 96/10, 372p.

Yu, Jiashun and A. J. Haines (1994). Observation and synthesis of seismic wavefields in basin structures -- Analysis of seismic wave amplification at Alfredton Basin, New Zealand, A report to the Earthquake Commission of New Zealand.

Yu, Jiashun and J. Haines (2000). The extremely high seismic amplification in Parkway, New Zealand (in preparation).